

Prediction of Water Vapor Concentration of Moist Air inside Batch Solar Dryers

ADRIAN GABRIEL GHIAUS^{1*}, YANNIS CAOURIS², VIOREL FATU¹

¹Technical University of Civil Engineering Bucharest, Thermal Engineering Department, 66 Pache Protopopescu Blvd., 021414, Bucharest, Romania

²University of Patras, Department of Mechanical Engineering and Aeronautics, Panepistimioupoli Rio, 265 04 Patras, Rio, Greece

Design optimization and evaluation of existing solar dryers can be done through numerical simulation of the complex and coupled transfer processes taking place inside drying units. Analysis of moisture concentration and relative humidity evolution of the drying air along with pressure, velocity and temperature profiles was done both inside the solar collector and drying chamber. Prediction of operation parameters for different design configurations allowed the identification of unwanted recirculation regions, saturation moist air zones and optimum operation time for an efficient drying process.

Keywords: water vapor concentration, air relative humidity, solar dryer, CFD analysis

For decreasing post-harvest losses in countrysides by small farmers, drying vegetables and fruits using solar energy is a common alternative. In food industry, preservation is one of the most important processes; while maintaining physical, biological and chemical properties of foods, it involves preventing the growth of micro-organisms such as bacteria and fungi. There are a lot of food preservation techniques, some of them very old and others very modern with really good results. However, not all of them are energy efficient and affordable for the small farmers. Drying, the oldest food preservation method, is one of the best means because the dried products preserve their taste and smell while cheeping their vitamins and nutrients almost untouched. The basic target of food drying is to remove water to a final concentration, which ensures microbial stability of the product and minimizes chemical and physical changes of the food during storage [1]. In the food drying, a rigorous control of operating parameters is important, aiming to maintain the biochemical and biological properties of the finite product [2]. Compared to other preservation methods, drying is not a complicated technique, dried products don't need any other additives (salt, sugar, anti-microbial liquid or artificial additives) that are also changing the products properties to preserve them and storage rooms, except low humidity levels, don't need to have a controlled environment. On the other hand, drying the products leads to the reduction of their volume and weight, minimizing packaging, storage and transportation costs [3]. With all the above-mentioned advantages, one can certainly say that solar drying is one of the best methods for food preservation. The most frequent problem of this technique is the uneven air flow and temperature profile which implies uneven humidity distribution inside the drying chamber and reduction of product quality. To verify the functionality and to optimize the parameters of the solar drying process, Computational Fluid Dynamics modeling techniques have been adopted by using Comsol Multiphysics code.

Experimental part

Materials and methods

The analyzed dryer is an indirect solar dryer made from two components, a solar collector and a drying chamber,

it has a simple design which ensures reduced construction cost and time and good functionality having a simple geometry which ensures a good air flow. The dryer's functionality relies entirely on solar energy since it doesn't use any electrical equipment (such as fans or alternative heat source). The solar collector is made from a wooden frame having at the bottom a metal plate absorber painted in black with an active surface of 1.2 m² and at the upper side, a transparent cover. The air is flowing upwards as its density decreases with the rise of temperature. The drying chamber is made entirely from wood having a total volume of 0.216 m³ and includes 5 detachable trays with 0.24 m² surface each one and 10 cm distance between them [4]. The dimensions of the dryer, in centimeters, are presented in figure 1. The chimney has a damper that can decrease the air flow up to zero as needed. For this study, the damper was set to fully opened position during the simulation of an entirely sunny day.

The simulation has been made on a reduced 2D model neglecting any end effects from the side walls in the third dimension. The domain was divided into finite elements with smaller dimensions on the aria with high gradient of temperature, velocity or humidity like the absorbent plate of the solar collector or near the trays. The created mesh using triangle (advancing front) method comprise 7459 elements and is presented in figure 2. The set of equations has been solved for all these elements but the results are presented only for the drying chamber domain where the coupled processes like momentum, heat and mass (water) transfer take place as well as water evaporation.

The unsteady-state simulation was carried out for a full sunny day starting at 6 AM and ending at 10 PM. Solar radiation, temperature and relative humidity of the atmospheric air are functions of time generated from meteorological data [5] as can be seen in figure 3. The intensity of solar radiation increases from 6 AM to 3 PM where it reaches the maximum value of 405 W/m² and then decreases up to zero near 9 PM. Outdoor air temperature varies from 20 to 29.8°C and relative humidity of atmospheric air takes values between 31% and 50%.

Simulation of the complex coupled processes that take place inside the dryer requires four modules, each one having its own set of equations, from the Comsol

* email: adrian.ghiaus@utcb.ro; Phone: +40 747 832 173

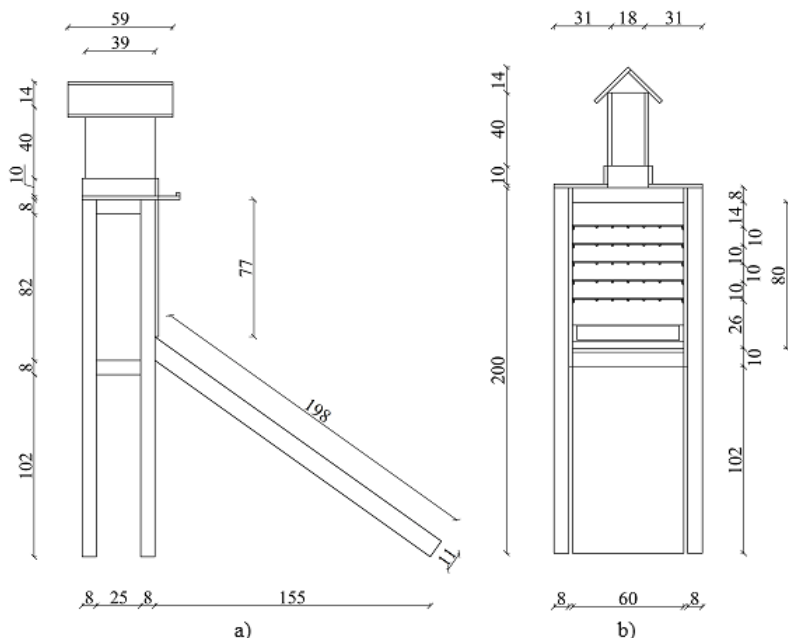


Fig. 1. Dimensions of the dryer: a) side view; b) back view

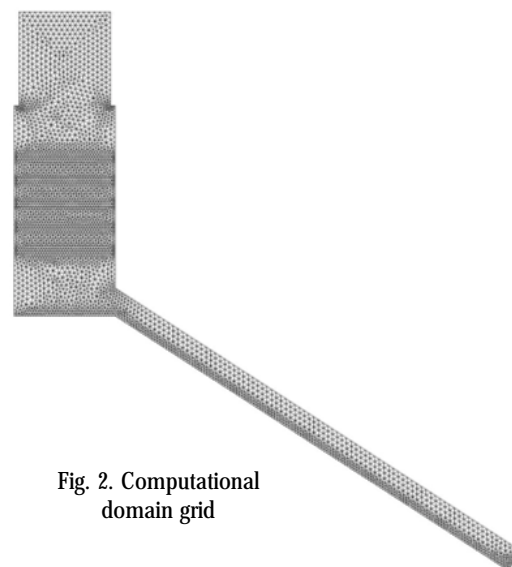


Fig. 2. Computational domain grid

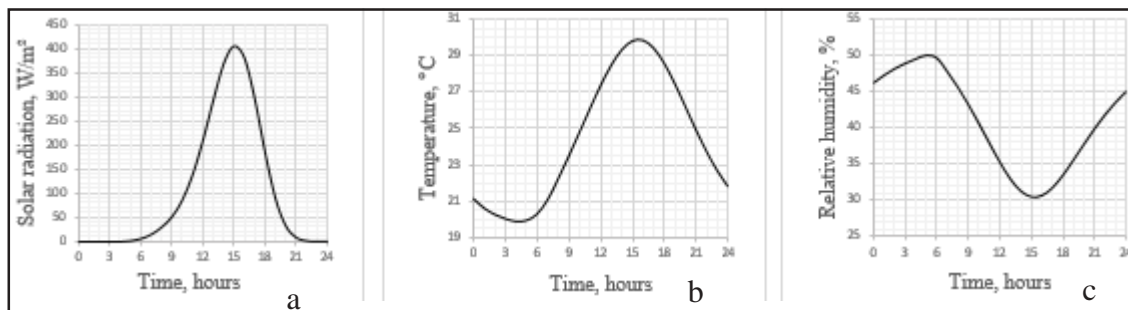


Fig. 3. Time-dependent solar radiation (a), temperature (b) and relative humidity (c)

Multiphysics library, i.e.: (1) *general heat transfer module*, which gives the solution for temperature field by solving, for each finite element, the heat equation; (2) *Brinkman equations module*, used to model the air flow through the product bed considered to be a porous media, by solving the Brinkman's momentum equation for every finite element belonging to the product tray; (3) *k-ε turbulence module*, responsible for simulation of the air flow by computing the solutions of Navier-Stokes equations with k-ε enclosure; (4) *convection and diffusion module*, loaded to enable the simulation of water evaporation and to determine the concentration of water vapor in air by solving the diffusion equation [6]. It was later used to compute the distribution of air relative humidity inside the drying room.

The heat equation, also called the energy conservation equation, states that the sum between thermal energy variation and divergence of the diffusive heat flux is equal to the heat generation rate [7]:

$$\rho \cdot c_p \cdot \left(\frac{\partial T}{\partial t} + \vec{w} \cdot \nabla T \right) + \nabla \cdot (-k \cdot \nabla T) = \dot{Q}_v \quad (1)$$

where ρ is the density in kg/m^3 , c_p is the specific thermal capacity at constant pressure in $\text{J/kg}\cdot\text{K}$, T is the temperature in K, k is the thermal conductivity in $\text{W/m}\cdot\text{K}$, t represents the time in s, \vec{w} is the velocity vector in m/s and \dot{Q}_v denotes the heat source flux in W/m^3 .

The trays, containing the product to be dried, are considered to be a porous medium subdomain, with high porosity and high permeability, for which the determination of the velocity field was done by solving the Brinkman equations, an extension of Darcy's law which accounts for shear induced momentum transfer [8]:

$$\rho \frac{\partial \vec{w}}{\partial t} - \nabla \cdot \mu (\nabla \vec{w} + (\nabla \vec{w})^T) - \left(\frac{\mu}{\kappa} \vec{w} + \nabla p - F \right) = 0 \quad (2)$$

where μ denotes the dynamic viscosity in Ns/m^2 , κ is the permeability in m^2/s , p the pressure in N/m^2 and F the volume force term in N/m^3 . For free-convection problem, the force term, also called Boussinesq buoyancy term, accounts for the lifting force due to thermal expansion:

$$F = \rho_0 g \beta (T - T_0) \quad (3)$$

where ρ_0 gives the reference density in kg/m^3 , g is the gravity acceleration in m/s^2 , β the thermal expansion coefficient in K^{-1} and T_0 is the reference temperature in K. The boundary conditions for Brinkman equation near the walls are all no slip.

The Navier-Stokes equations for non-isothermal unsteady flow can be written as [9]:

$$\rho \frac{\partial \vec{w}}{\partial t} + (\vec{w} \cdot \nabla) \cdot \rho \vec{w} = -\nabla p + \mu \nabla^2 \vec{w} + \rho g \quad (4)$$

coupled with the continuity equation:

$$\frac{\partial \rho}{\partial t} + \nabla \cdot (\rho \vec{w}) = 0 \quad (5)$$

In k-ε turbulence model, the typical velocity is calculated from the solution of the transport equation for turbulent energy kinetic and dissipation rate [10]:

$$\frac{\partial (\rho k)}{\partial t} + \nabla \cdot (\rho \vec{w} k) = \nabla \cdot \left(\frac{\mu_t}{\sigma_k} \cdot \nabla k \right) + \rho (P_k + G_b - \varepsilon) \quad (6)$$

$$\frac{\partial (\rho \varepsilon)}{\partial t} + \nabla \cdot (\rho \vec{w} \varepsilon) = \nabla \cdot \left(\frac{\mu_t}{\sigma_\varepsilon} \cdot \nabla \varepsilon \right) + \rho \frac{\varepsilon}{k} (C_1 P_k + C_2 G_b - C_3 \varepsilon) \quad (7)$$

where $\frac{1}{2}\rho u'^2$ is the kinetic energy of turbulence, ε is the dissipation rate, μ_t is the dynamic turbulent viscosity, P_k and G_k are the volumetric production rates of turbulent kinetic energy by shear forces and by gravitational forces interacting with density gradients, respectively, $\sigma_k=0.9$ and $\sigma_\varepsilon=1.3$ are the effective Prandtl-Schmidt numbers and C_1 , C_2 and C_3 are constants determined from experimental data.

Relative humidity field is calculated from the concentration of water vapor in the moist air by solving the diffusion equation:

$$\frac{\partial c}{\partial t} - \nabla \cdot (D \cdot \nabla c) = R - \tilde{w} \cdot \nabla c \quad (8)$$

where c stands for water vapor concentration in mol/m^3 , D is the diffusion coefficient in m^2/s , R is the evaporation rate of water from the product in $\text{mol/m}^3 \cdot \text{s}$.

For the humid air, the diffusion coefficient was set to the value $D=2.6 \times 10^{-5} \text{ m}^2/\text{s}$. Inside the product bed, since it is considered a porous media, the diffusivity was adjusted using the Bruggeman correction:

$$D' = \varepsilon_p^{3/2} \cdot D \quad (9)$$

where ε_p stands for the correction coefficient.

In this study, the physical properties of the drying air were calculated using the analytical formulas for dry air since most properties, like density and dynamic viscosity, have similar values for dry and moist air. The functions describing the properties of dry air are loaded when selecting air from the Comsol material/coefficients library; for example, air density is obtained from the ideal gas equation and it has the following expression:

$$\rho = \frac{P}{R_a(T + 273.15)} \quad (10)$$

where R_a is the air specific constant in $\text{J/kg} \cdot \text{K}$ and is defined as the ratio between the ideal gas constant, R in $\text{J/mol} \cdot \text{K}$ and the molar mass, M in kg/mol :

$$R_a = \frac{R}{M} = \frac{8.314}{0.02897} = 286.986 \text{ J/kg} \cdot \text{K} \quad (11)$$

Since the dryer does not use any fan or other working equipment, the air movement entirely relies on free convection driven by the density gradient. The volume force component on the vertical direction, F_v was calculated as the product between the difference in air density (inside - outside) and the gravitational acceleration:

$$F_v = (\rho - \rho_0) \cdot g \quad (12)$$

where ρ is the density of the air inside the dryer in kg/m^3 and ρ_0 denotes the density of the surrounding air in kg/m^3 .

The air density inside the dryer, ρ , is automatically calculated with relation (10) and using the same relation, the density of the outside air ρ_0 is computed by setting the temperature to take values according to the function of time generated from experimental data so that the surrounding air density also becomes a function of time.

Evaporation process is taken into account by considering the mass of water that is evaporated from the products as the source term R in the diffusion equation. In order

evaporation to take place, the water vapor concentration at the product surface has to be greater than the water vapor concentration in the moist air, computed as:

$$c = \frac{\phi \cdot p_s}{R \cdot T} \quad (13)$$

where ϕ is the air relative humidity and p_s represents the saturation pressure in N/m^2 , calculated as a function of temperature using the following approximation [11]:

$$p_s = A \cdot 10^{\frac{7.5 \cdot (T - B)}{T - C}} \quad (14)$$

where the constants have the following values: $A=610.7 \text{ N/m}^2$, $B=273.15 \text{ K}$ and $C=35.85 \text{ K}$. Hence, the evaporated water mass rate is calculated as:

$$\dot{m}_{\text{evap}} = E \cdot (c_s - c) \quad (15)$$

where E stands for evaporation rate in s^{-1} , which value depends on the material properties and the process causing evaporation; for this case, having considered the product bed as a high porosity material, $E = 1 \text{ s}^{-1}$.

The heat loss by water evaporation from the product was inserted as a negative heat source using the following relation:

$$Q = -H_{\text{evap}} \cdot \dot{m}_{\text{evap}} \quad (16)$$

where H_{evap} represents the heat of vaporization (J/mol) equal with the product between the latent heat of vaporization and the molar mass of water:

$$H_{\text{evap}} = L_v \cdot M_w \quad (17)$$

with $L_v = 2.433 \cdot 10^6 \text{ J/kg}$, $L_v = 2.433 \cdot 10^6 \text{ J/kg}$, the latent heat of vaporization at the mean temperature of the product and $M_w = 0.018015 \text{ kg/mol}$, the molar mass of water.

The water vapor concentration in the air is obtained as the product between the mole fraction of water vapor in moist air and the molar air density:

$$c_v = x_v \cdot \rho_m \quad (18)$$

The mole fraction of water vapor in moist air is calculated as the partial pressure of water divided by the total pressure of air considered at normal conditions $p_o = 101.3 \text{ kN/m}^2$:

$$x_v = \frac{p_v}{p_o} \quad (19)$$

The partial pressure of water vapor is calculated based on the saturation pressure of water and the time dependent relative humidity of outside air generated from meteorological data:

$$p_v = p_s \cdot \phi_s \quad (20)$$

The molar density, in mol/m^3 , can be calculated with the following relation:

$$\rho_m = \frac{P}{R \cdot (T + 273.15)} \quad (21)$$

Results and discussions

The four modules, i.e. general heat transfer, k- ε turbulence, Brinkman equations and convection and diffusion, were loaded in Comsol Multiphysics and the above mentioned equations were set for each specific

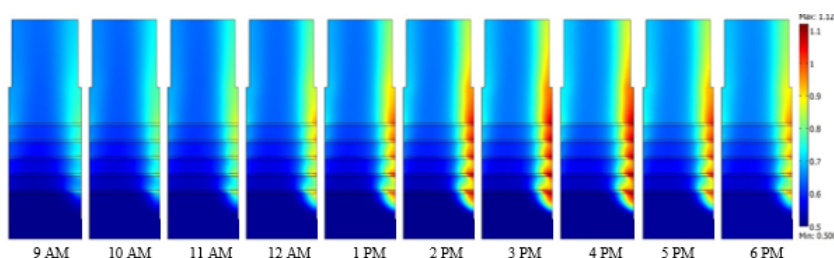


Fig. 4. Water vapour concentration in mol/m^3 from 9 AM to PM

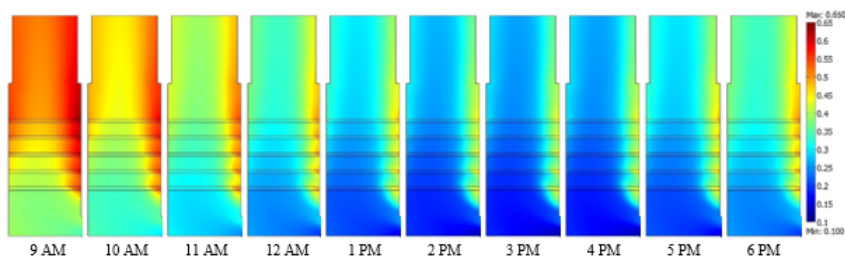


Fig. 5. Relative humidity distribution from 9 AM to 6 PM

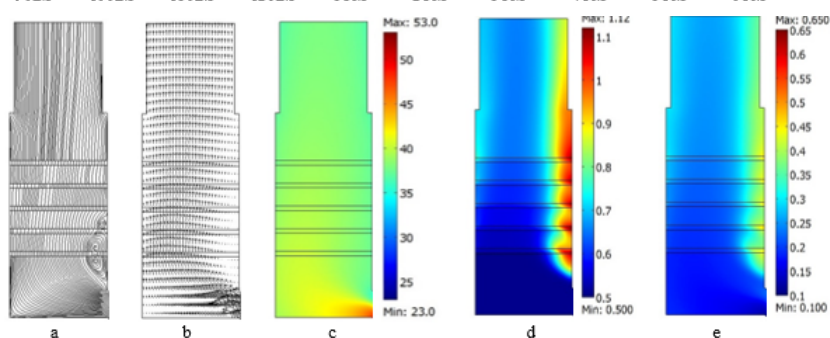


Fig. 6. Analysis of drying air parameters at 3 PM
a - streamlines; b - velocity; c - temperature;
d - concentration; e - relative humidity

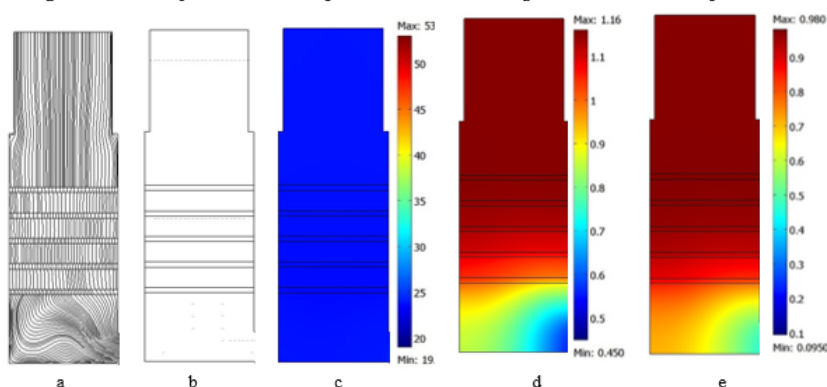


Fig. 7. Analysis of drying air parameters at 10 PM
a - streamlines; b - velocity; c - temperature;
d - concentration; e - relative humidity.

subdomain. All boundary conditions were specified, transient study was selected and the time was set to start from $t=0s$ (corresponding to 6AM) and to stop after 16 h, at $t=57600s$ (corresponding to 10PM). The results for the space distribution of streamlines, velocity, temperature, concentration and relative humidity inside the drying space have been obtained at different hours [12]. Since for the first three hours (startup period) and the last four hours the solar radiation is very low or even zero, only the time interval from 9AM to 6PM was chosen to be presented.

Concentration of water vapor in drying air inside the drying room is presented in figure 4. During the entire period, but especially in the afternoon when solar radiation and ambient temperature have higher values, water vapor concentration increases near the front wall (the side where solar collector is attached). This is due because the air flow is less intense and recirculation also appears. A higher concentration of water vapor in the drying air will negative affect the drying rate and therefore in these regions the product will need more time to reach the desired final moisture content.

Relative humidity of the drying air depends on both air temperature and water vapor concentration. The increase of drying air temperature during the day will reduce relative humidity while the water evaporation from the product will raise its value. However, the saturation limit is far from being achieved. The relative humidity distribution is presented in figure 5. It can be seen that in general, relative humidity has values below 50%, which means that the capacity of the drying air to take away the evaporated water from the product is high enough. The same as in concentration distribution, near the front wall it can be observed higher values of relative humidity.

The optimal environment conditions for drying are achieved around 3 o'clock in the afternoon when the

intensity of solar radiation is $400W/m^2$, the temperature is $30^{\circ}C$ and the relative humidity is 30%. Figure 6 presents the drying air parameters (streamlines, velocity, temperature, concentration and relative humidity) inside the drying room. Recirculation associated with low velocity can be observed near the front wall and this affects in a negative way the drying rate in this small region. Air temperature is quite uniform, around $40^{\circ}C$, however concentration and relative humidity tend to grow near the front wall.

After the sunset, when air circulation inside the dryer is progressively reduced, the water evaporated from the product is no longer taken out and the relative humidity starts to increase until it reaches the saturation point around 10PM. Drying becomes inefficient and measures should be taken in order to avoid this situation. Drying air parameters at 10PM are shown in figure 7. The velocity vector field is almost zero, temperature decreases near ambient value and relative humidity tends to the maximum.

Conclusions

Unsteady convective drying process was numerically modeled for the case in which solar radiation was the only source for heating the drying air. Specific functions for ambient time-depending parameters as temperature, relative humidity and intensity of solar radiation were proposed. The coupled partial differential equations were solved by finite element method using Comsol Multiphysics commercial code. The model was applied on an indirect solar dryer with appropriate design based on low-costs and easy accessibility to manufacturing resources.

CFD, one of the best tools in design optimization, gives the opportunity to identify some possible problems regarding airflow while the measurements taken in-situ

show similar results for the temperature and the relative humidity values. Although the dryer has a simple geometry and does not use any high technology equipment, the coupled processes involved in drying based on complex phenomena lead to high requirements of internal memory and computing time. Prediction of operation parameters allows the identification of unwanted recirculation regions, saturation moist air zones and optimum operation periods for an efficient drying process.

References

1. ISOPENCU, G., MARES, A.-M., JINESCU, G., Rev. Chim. (Bucharest), **68**, no. 6, 2017, p.1274
2. JINESCU, G., MIHAILESCU, D.-M., ISOPENCU, G., MARES, A.-M., Rev. Chim. (Bucharest), **60**, no. 6, 2009, p.616
3. KOTHARIS., PANWAR N. L., CHAUDHRIS., Int. J. Renewable Energy Technology, **1**, 2009, p.30
4. VINTILA M., GHIAUS A.-G., FATU V., Bulletin of USAMV Food Science and Technology, **71**, No. 2, 2014, p.189
5. LOWE P. R., FICKE J. M., Environmental Prediction Research Facility, 1974
6. GHIAUS A.-G., FATU V., Proceedings of 5th European Drying Conference, EuroDrying'2015, Vol. 1, 2015, p.125
7. COMSOL AB, Comsol Multiphysics User's Guide, 2006
8. RIECK R., BENARD A., PETTY C., Proceedings of the COMSOL Conference, 2009, CD-ROM
9. COMSOL AB, Heat Transfer Module User's Guide, 2006
10. MARGARIS D., GHIAUS A.-G., J. Food Eng., **75**, 2006, pp.543-544
11. MONTEITH J. L., UNSWORTH M. H., Principles of Environmental Physics, Butterworth-Heinemann. Oxford, 1990
12. GHIAUS A.-G., MARGARIS D.P., FATU V., Proceedings of 7th International Conference from Scientific Computing to Computational Engineering (7th IC-SCCE), 2016, pp. 303-305

Manuscript received: 17.11.2017